Sol–gel coatings for protection and bioactivation of metals used in orthopaedic devices

A. Durán,[a] A. Conde,[b] A. Gómez Coedo,[b] T. Dorado,[b] C. García[c] and S. Ceré[d]

[a]Instituto de Cerámica y Vidrio (CSIC), Campus de Cantoblanco, 28049 Madrid, Spain
[b]Centro Nacional de Investigaciones Metalúrgicas (CSIC), Gregorio del Amo 8, 28040 Madrid, Spain
[c]Universidad Nacional de Colombia sede Medellín, A.A. 3840 Medellín, Colombia
[d]Instituto de Investigaciones en Ciencia y Tecnología de Materiales. UNMdP-CONICET, Juan B., Justo 4302, B7608FDQ Mar del Plata, Argentina

The aim of this work is the production and characterisation of sol–gel coatings for protection and bioactivation of metals used as standard surgical implant materials, such as stainless steel 316 L (ASTM F138), Co based alloys (ASTM F75) and titanium alloy Ti-6Al-4V (ASTM F67). These films should both prevent degradation of the substrates by wear or corrosion, and bioactivate the material for inducing the formation of a hydroxyapatite (HA) rich layer onto the material surface, thereby permitting a natural bonding to living tissues. Formation of HA layers can be observed on performing in vitro tests by soaking the material in simulated body solutions. The work describes the development of coatings containing bioactive glass and glass-ceramic particles in hybrid methyl-triethoxysilane (MTES) and tetraethylorthosilicate (TEOS) acidic sol, applied by dip-coating to surgical alloys, AISI 316 L, ASTM F75 and ASTM 67, with the aim of accomplishing both high corrosion resistance of the metal in the body environment and adhesion of the implant to the surrounding tissue. The performance of the coated metal was evaluated in vitro by electrochemical techniques including potentiodynamic polarisation curves and electrochemical impedance spectroscopy, to follow the formation of hydroxyapatite on the surface, as well as the in vitro release of ions by plasma atomic emission spectroscopy (ICP-MS) after up to one year of immersion. In vivo behaviour was evaluated by subcutaneous tests and endomedullar implantation in Hokaido rats to study possible rejection reactions and natural bonding to living tissue.

1. Introduction

Biomedical prosthetic devices are used in the human body to carry out the functions no longer performed by the original parts. Metals are used in the human body mainly for orthopaedic purposes and their degradation by wear and/or corrosion must be negligible. Standard surgical implant materials include stainless steel 316 L (ASTM F138), Co based alloys (mainly ASTM F75, and F799) and titanium alloys; where Ti-6Al-4V (ASTM F67 and F136) are the most employed. The use of these alloys for orthopaedic appliances requires the formation of a passive film to prevent oxidation. These films consist of metal oxides which form spontaneously on the metallic surface to limit the transport of metal ions across the metal oxide–solution interface. These films should not only be non-porous and fully cover the metal surface but must also remain on the surface under mechanical stresses. In addition the surface should allow repassivation in case of film removal or damage.[1]

Cobalt based alloys are widely used for fabrication of diverse surgical devices due to their good corrosion and wear resistance as well as their good biocompatibility. The main corrosion products, CoO and Cr_2O_3, may react with water to form Co(OH) and $Cr(OH)_3$.[2] Cell culture has demonstrated that chromium species can stimulate osseous resorption and necrosis of periprosthetic tissue.[3]

Titanium alloys are employed for orthopaedic implants due to their excellent combination of biocompatibility, corrosion resistance and mechanical properties. However, toxicity of alloying elements and a high elastic modulus compared to bone have been reported as possible disadvantages.[4] Although titanium has excellent corrosion resistance, if any of the alloying elements are released into the tissue by corrosion or wear, tissue reaction may vary, ranging from a mild response, such as the discoloration of surrounding tissue, to a severe one causing pain and even loosening of the device.[5]

AISI 316L stainless steel is widely used in applications where the implant is temporary, although it is also employed for permanent implants. However, it tends to localised corrosion releasing significant quantities of iron ions to the neighbouring tissues with the consequent risk of local tumours and mechanical failure of the implant.[6,7]

For permanent prosthesis and especially for joint replacement, it would be desirable to avoid cementing of prostheses by promoting natural bonding to hard and soft tissues.[8–11]

Uncemented prosthetic components with porous surfaces are increasingly used in total joint replacement surgery for young and active patients.[12] However, for this kind of patient, who may have a postoperative life expectancy of more than thirty years, the carcinogenic potential of metal elements used in total hip arthoplasty components is a great concern, particularly because of the high exposed surface of porous devices inserted without cement.[1]

One way to minimise the release of corrosion products from the implant to the surrounding tissue is to apply protective coatings. Such films should also be functional with bioactive material for inducing the formation of a semi-crystalline hydroxyapatite (HA) rich layer onto the material surface, generating a natural bond to living tissues. HA can be detected after in vitro tests performed by soaking the material in simulated body solutions (SBF), Hank's balanced salt solution (HBSS), and other solutions that simulate body

fluids.[13–15] This behaviour is considered an indication of *in vivo* bioactivity.[16–18]

The sol–gel method has been proposed as a suitable procedure to produce protective[19–21] and bioactive[22,23] coatings. The advantages and technological significance of these sol–gel coatings over those produced by other methods have been widely demonstrated.[24–26] One of the most attractive characteristics of the sol–gel method is that through the use of different precursors, thermal treatments, or addition of particles in the sol, functional coatings can be obtained. Sol–gel processing has been employed to some extent for preparing bioactive glasses and gels.[27–32] The range of bioactivity in the $CaO–SiO_2–P_2O_5$ system is larger for bulk materials prepared by sol–gel than for the same glass compositions obtained by melting.[31] Some porous SiO_2 gels also show *in vitro* induction of HA deposition.[33] However, crack-free coatings for compositions showing bulk bioactivity (16% CaO, 4% P_2O_5, 80% SiO_2)[30] prepared by using calcium methoxide, triethylphosphate and TEOS as sol precursors,[21] showed no *in vitro* formation of HA after 1 month of immersion in SBF. Differences between sol–gel bulk and film behaviour can be attributed to the higher density of coatings,[34] which limits their reactivity.

Galliano and co-workers demonstrated that inorganic and hybrid SiO_2 coatings obtained from tetraethylorthosilicate (TEOS) and/or methyltriethoxysilane (MTES) as SiO_2 precursors using acid catalysts improve the corrosion behaviour of AISI 316L stainless steel in biological environments.[21] Coatings were applied as mono and multilayers by a multistep method. XPS analysis of inorganic and hybrid SiO_2 coatings on steel substrates showed that using TEOS as the only precursor results in some extent of Fe diffusion, but the hybrid coatings prepared from MTES/TEOS limited the diffusion of iron to surface during thermal treatment, with much lower iron contents than those reported for bioactivity inhibition.[35]

This work describes the development of sol–gel coatings containing bioactive glass and glass-ceramic particles in hybrid silica matrices, applied by dip-coating to surgical alloys including ASTM F75, ASTM F 67 and AISI 316 L. The deposition of these coatings has two main objectives: the reduction of corrosion of the substrates in the body and stabilization of the implant (without the use of cement), allowing the growth of new osseous tissue around the insert. The performance of the coated metals was evaluated *in vitro* by following the formation of hydroxyapatite on the surface using electrochemical techniques. In addition, *in vitro* ions release was measured by mass plasma atomic emission spectroscopy (ICP-MS) after long periods of immersion. *In vivo* behaviour was evaluated by subcutaneous and endomedullar implantation in Hokaido rats.

2. Experimental

2.1. Synthesis of silica sol and suspensions

Tetraethylorthosilicate (TEOS) and methyltriethoxysilane (MTES), both from ABCR, were selected as SiO_2 precursors for the hybrid sol (sol HS), prepared in alcoholic media using HNO_3 and acetic acid as catalysts. A molar relationship MTES/TEOS of 60/40 was employed, fixing R = 2, where R = H_2O/(MTES + TEOS). The final concentration of SiO_2 was 200 g l^{-1}.

The bioactive glass belongs to the $CaO–SiO_2–P_2O_5$ system with 57.44 CaO, 35.42 SiO_2 and 7.15 P_2O_5 in molar percentages. Silica sand with low Fe_2O_3 content, CO_3Ca (Panreac) and POH_3 (Merck) were used as raw materials. The glass was obtained by melting the batch at 1600 °C for 2.5 hours then quenching in water at room temperature.[35,23] Bioactive glass-ceramic particles were obtained from this glass employing a heat treatment for 2 hours at 1050 °C to induce crystallization of hydroxyapatite and wollastonite. All the bioactive particles were milled in a planetary mill (Fritsch Pulverisette, Germany), with agate jar and balls at 1500 rpm for a maximum period of 1 h. After milling, the powders were sieved, using Tyler sieves numbers 270 (54 μm), 325 (43 μm), 400 (37 μm) and 600 (25 μm). Different fractions were selected to analyse the influence of particle size on the coating behaviour. The particle size distribution and the specific surface area were determined by laser diffraction and N_2-adsorption BET.

Stable suspensions were obtained by adding 5 and 10 wt% of particles to the hybrid silica sol. Three different particle sizes were used for studying the kinetics of reaction *in vivo* and *in vitro*. Suspensions with small bioactive particles of diameter around 5 μm were prepared by using phosphate ester (Emphos PS21, Whitco Chem, USA) as processing additive and further addition of citric acid to obtain a suitable pH. Larger particles of glass ($\phi \approx 39$μm) and glass-ceramic ($\phi \approx 17$μm) were also employed for preparing stable suspensions by using tetrapropyl ammonium hydroxide (TPAH, Aldrich) in a concentration of 50 wt% with respect to solids.

The stability of the suspensions was evaluated by measuring the viscosity as a function of time. Rheological measurements were performed using a rotational rheometer (Haake RS50, Germany) with a double-cone and plate-measuring system.

2.2. Substrates and coatings

Three alloys were studied: CrCoMo alloy (ASTM F75), Ti 6Al 4V (ASTM F68) and stainless steel AISI 316L. Plane sheets of cast CrCoMo alloys (F75 alloy, Zimmer Inc.) of around 2 cm^2 were cut and polished with emery paper and alumina (0.3 μm) until a mirror finish was achieved. Wires of 1.4 mm diameter of CrCoMo alloy (Zimmer Inc.) were also made by polishing at one end in order to obtain a needle-like shape to improve the deposition of the sol and increase fixation in the *in vivo* studies. Samples were cleaned in an ultrasonic bath and dipped in isopropyl alcohol prior to coating. Plates (25mm × 50mm) and surgical nails ($\phi = 1.5$ mm) of as-received AISI 316L stainless steel (average roughness, $R_a \geqslant 2$) were also employed. Cleaning was performed with the following schedule: 5 min in alkaline bath (demineralised water : P3 Emalan 5668 : P3 Emalan 0469 = 1000 : 50 : 5) at 60 °C, 1 min in demineralised water at room temperature and 1 min in demineralised water at 60 °C. Titanium plates of 35 × 50 mm were used as-received and cleaned in the same manner.

The metallic substrates were coated by dipping to obtain mono and double-layer coatings. Single coats were obtained from the glass and glass-ceramic/hybrid sol suspensions, as well as from the pure hybrid silica sol, and thermally treated at 450 °C for 30 min in air. The double-layer coatings were prepared in two steps, with a first inner film obtained from the hybrid SiO_2 sol, heat-treated with the same schedule. The second layer, deposited from the suspensions with bioactive particles, were thermally treated again at 450 °C for 30 min. Coatings were also applied onto glass-slides for thickness measurements, performed with a mechanical profilometer Talystep (Taylor–Hobson). Mono and two-layer coatings were controlled by optical microscopy (Olympus BX41).

The concentration of the particles in the coatings was calculated by obtaining a digital image of each coating in an optical microscope (Olympus BX-41) using a video system consisting of a CCD sensor connected to an acquisition card IMAQ-PCI-1408 (National Instruments, TX, USA) in a PC IBM, controlled by software developed in LabView 5.1. (National Instruments, TX, USA) and Matlab 5.3 (MathWorks, Inc., MA, USA). The software enhances the contrast of the image to clearly distinguish the particles from the matrix and afterwards calculates the concentration of each phase present.

2.3. *In vitro* assays

In vitro assays were conducted either in simulated body fluid (SBF)[13] at 37 °C, pH 7.3 ± 0.1, prepared with bidistilled water grade I (Millipore) or in commercial Hank's balanced salt solution (HBSS, SIGMA). Electrochemical experiments were performed using electrochemical units (Solartron 1280B and Gamry CSM 100). A saturated calomel electrode (SCE) (Radiometer) was used as reference electrode and a platinum wire was used as secondary electrode. Impedance experiments (EIS) were conducted at the corrosion potential (E_{corr}) with an amplitude of 0.005 V r.m.s; frequency was swept from 100 kHz to 0.01 Hz. Potentiodynamic polarisation curves were collected applying a cathodic potential step of 300 mV with respect to the E_{corr}; the anodic sweep at 0.002 V s^{-1} starts from this value up to 1.2 V *versus* SCE where the reverse scan initiates.

In vitro bioactivity tests were performed on coated samples by immersion in HBSS at 37 °C during different periods of time, with a ratio between the sample area and the fluid volume of 0,4 cm ml^{-1}. Deposition of apatite, the bone mineral phase, onto the surface of the coatings, considered as a preliminary signal of bioactivity,[13] was followed by specular reflection infrared spectroscopy (FTIR), X-ray diffraction (XRD) and scanning electron microscopy (SEM).

Ion release in simulated body fluids has been studied with ICP-MS for long-term tests of up to one year. Samples were immersed in narrow glass tubes containing the minimum SBF solution to totally cover the sample surface and maximise the concentration of released ion. The average volume of SBF in contact with each sample was 19 ml. Solutions were analysed, on soaking from one month to one year depending on the substrate together with a reference SBF bath (without sample). Tests were performed at 5 and 37 °C to confirm the stability of the solution.

2.4. *In vivo* assays

In vivo experiments were conducted with Hokaido rats. Subcutaneous tests were performed with the aim of testing the possible rejection reactions. Three animals were implanted with square (15 mm × 15 mm) coated and uncoated plates in the muscle dorsal area. Implantation was performed under sterile conditions and plates were situated under the skin, contacting the muscle fascia. After one month, the animals were sacrificed and the implanted material with the surrounding tissues was extracted.

For endomedullar studies, coated and uncoated wires were sterilised by dry heat in an electric oven (Hogner) over a period of one hour at 160 °C. CrCoMo wires of $\phi = 1.4$ mm, 3–4 cm in length were placed in the tibia cortical bone of five animals. The implants were inserted while the rats where sedated under 1 ml Innovan (Janssen Lab., droperidol and fentanyl citrate) anaesthetic. The animals were placed in a supine position and painted with a colourless antiseptic. The implantation site was exposed through the superior part of the internal face of the tibia. A region of around 5 mm diameter was scraped in the tibia plateau to prepare the burring area. A hand drill with a 1.5 mm bur was used at low rotation rate (120 ± 10 rpm). The implantation site was irrigated with physiological saline solution for cooling and cleaning purposes during the drilling procedure and before the implant was inserted. The coated and uncoated wires were located by a press fit technique in both tibias of the rat, extending into the medullar canal. The wound was closed with conventional suturing. The rats were sacrificed with an overdose of intraperitoneal Innovan after 53 days and X-rayed before retrieving the tibia. The retrieved sections were examined for the presence of bone/sol–gel coating interface and bone/alloy interface. Each rat had one uncovered wire in one tibia bone and a coated wire in the other tibia. The material was placed in neutral formol. Osseous tissue was decalcified and multiple cuts at various levels were made to improve fixation. The material was cut on a microtome, stained with haematoxylin and eosin and observed by an optical transmission microscope (Leica DLM); photographs were taken and analysed by a viewer (Leica DC Viewer).

3. Results and discussion

### 3.1. Characterisation of sols, suspensions and coatings

Stable glass/hybrid sol suspensions with non-agglomerated powders, necessary for obtaining homogeneous and crack-free layers, were prepared from differently sized particles. The best results for small glass particles ($\phi_m = 5$ μm, $S_e = 3$ m^2 g^{-1}) were obtained by using 0.1 wt% (referred to dry solids) of phosphate ester, adjusting the suspension pH to 3.8 by adding citric acid. The suspensions were stable for several days. Some sedimentation was observed when stored without agitation, but was easily re-dispersed on stirring. Viscosity showed neither significant variation with glass content, nor with storage time (up to one week), maintaining a value between 2–3 mPa s in all cases. The phosphate ester was first added to promote its adsorption onto the particle surfaces, acting as an anionic surfactant.[36] This affects the sol by raising the pH, so that a further acid addition is needed to prevent destabilization of the sol.[35]

In the case of larger particles ($\phi = 40$ μm, $S_e = 0.3$ m^2 g^{-1} for glass, and $\phi = 16$ μm, $S_e = 0.8$ m^2 g^{-1} for glass-ceramic powders) stability was obtained by adding TPAH, which raises the suspension viscosity up to 7 mPa s; the stability is maintained for 8 hours. TPAH acts as a cationic surfactant which is adsorbed on the particles; it also increases the pH to 6–7, so that the solution is far from the isoelectric point and electrostatic repulsion among the particles is favoured.[37]

The coatings obtained from the suspensions containing glass and glass-ceramic particles are composed of a glassy matrix with a secondary phase of particles with a concentration of 10–15 vol%, depending on the withdrawal and evaporation rates. The embedded particles appear separated showing a uniform distribution throughout the coatings, which demonstrates the stability and homogeneity of the precursor suspensions during the process. Fig. 1 shows a typical homogeneous and defect-free distribution of small glass particles (a) and medium size glass-ceramic powders (b) in the hybrid silica matrix. The critical thickness is between 1.5 and 3 μm depending on the particle size; in both types of coatings, some defects and cracks appear for thicker films. The inner hybrid silica coating was 1 μm thick, and the double layer thickness was between 2.5 and 3 μm.

3.2. *In vitro* electrochemical assays

Electrochemical tests showed that the presence of coatings always improves the corrosion resistance of all the metallic substrates. Fig. 2a shows typical polarisation curves for as-received and mono and double-layer coated F75 alloy in neutral SBF solution. It is observed that the alloy remains passive over a broad potential range before the breakdown potential (E_r) is reached. The protection potential was found to be 0.11 V positive to the open circuit potential. Thus, once the failure is initiated, re-passivation would be difficult since the protection potential is quite close to the corrosion potential. Degradation would then proceed, causing emission of undesirable corrosion products to the environment. The general shape of the polarisation curve for the bare alloy is similar to that of pure chromium. It has been previously demonstrated that the passive film is composed of chromium and/or cobalt species such as $Co(OH)_2$ and Cr_2O_3, which is partially converted to $Cr(OH)_3$.[2] The deposition of the hybrid coating decreases the passive current density for all the studied coatings. Although
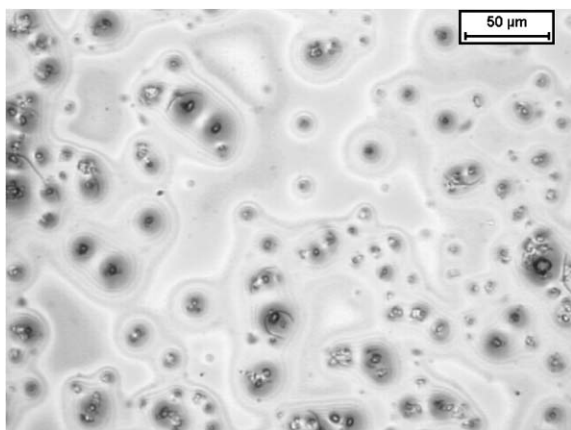
a)
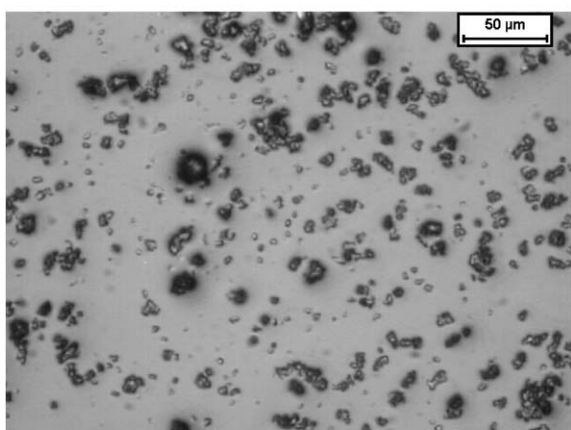
b)

Fig. 1 Optical microscopy photographs of double layer coatings: (a) with small glass particles (medium $\phi \approx 5\mu m$) and (b) with intermediate glass-ceramic particles (medium $\phi \approx 16\ \mu m$).

(a)

(b)

Fig. 2 (**a**) Potentiodynamic polarisation curve for the coated and uncoated CrCoMo alloy (F75) in neutral SBF solution, $v = 0.002\ \mathrm{V\ s^{-1}}$. (a) Double-layer coating with 5 wt% glass-ceramic; (b) Single layer with 5 wt% glass-ceramic; (c) Double-layer coating with 10 wt% glass-ceramic; (d) Single layer with 10 wt% glass-ceramic; (e) uncoated CrCoMo alloy. (**b**) Potentiodynamic polarisation curve for the coated and uncoated CrCoMo alloy in acidic SBF solution, $v = 0.002\ \mathrm{V\ s^{-1}}$. (a) Double-layer coating with 10 wt% glass-ceramic; (b) Single layer with 10 wt% glass-ceramic; (c) uncoated CrCoMo alloy.

there are no changes in the breakdown potential, the protection potential shifts 0.5 V positive to the corrosion potential, suggesting that this system is more likely to repassivate when the film is damaged. The differences found in the current density of coatings containing 5 and 10 wt% of powder may be due to particle agglomeration caused by the higher concentration. This may induce the appearance of microcracks during heating and/or cooling after densification. After 30 days of immersion in SBF, the passivation current density of the coated samples is still lower than that of coated samples, indicating that the sol–gel film deposited on the surface is preventing corrosion.[38] Although the current density presented for the coated samples showed an increase with potential, it was always lower than that of the uncoated samples. Therefore, around E_{corr}, the corresponding density current is more that two orders of magnitude lower for coated samples than for the uncoated samples.

As cobalt-base alloys are susceptible to crevice attack, coated pieces were tested in SBF acid solution (pH 0.7) in order to simulate the acidic media and the high chloride concentrations that develop when a crevice is formed. This attack could take place when partial scaling of the coating occurs. In acidic solution, the surface of the bare alloy is passive with low density currents until the breakdown potential is reached, as observed in Fig. 2b). The potential protection for the bare alloy in acidic SBF is around 0.1 V and seems not to improve for coated samples. Nevertheless, both the bare and the coated alloy showed low passive current densities that remained very stable within a broad potential range (1.3 and 1.1 V for the coated and uncoated alloy respectively). Thus, it is likely that
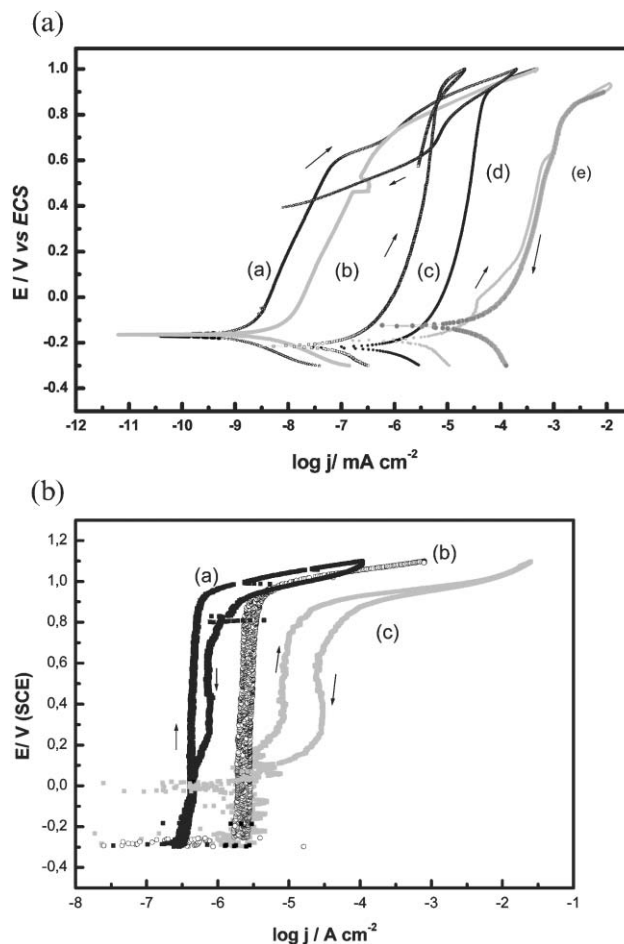
these systems present good ability for re-passivation in acidic solution and an acceptable localised corrosion resistance.

Fig. 3 shows potentiodynamic polarisation curves for Ti-6Al-4V with single and double layers with 10 wt% of glass particles compared with the uncoated metal. The anodic reverse scan corresponding to the alloy Ti-6Al-4V occurs at lower current densities due to the growth of a protective oxide layer during the anodic sweep. It can be observed that the coating drastically reduces i_{pass}, and it is probable that the sol–gel coating is also blocking active sites, reducing the effective electroactive area. Moreover, no change in the potential breakdown E_r was observed. This potential can be defined as that where a continuous increase in the anodic current under potentiodynamic control implies localised corrosion, either through pitting or crevice corrosion or transpassivation. This behaviour, together with the fact that the E_{corr} values are the same as that of the uncoated substrate, suggests there is open porosity, which leaves the alloy in contact with the solution. Thus, exposed substrate oxidises as the uncoated Ti-6Al-4V does, but over a much smaller area; consequently, the current density is also lower. Impedance measurements also indicate that the coating is porous.

Fig. 4 shows the evolution of the impedance spectra of a monolayer with 10 wt% of glass particles as a function of time. The spectra indicate the rapid disappearance of the coating
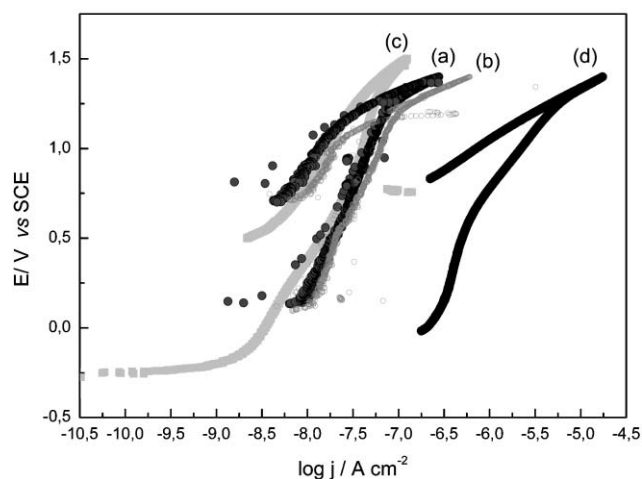
Fig. 3 Potentiodynamic polarisation curves for the coated and uncoated Ti-6Al-4V alloy in neutral SBF solution, $v = 0.002$ V s^{-1}. (a) Double-layer coating with 10 wt% glass; (b) Double-layer coating with 10 wt% glass-ceramic; (c) Single layer with 10 wt% glass; (d) Uncoated Ti-6Al-4V alloy.

Fig. 5 Potentiodynamic polarisation curves for (a) hybrid silica and (b) double layer with 10 wt% glass particles compared with (c) bare AISI 316L stainless steel.

response with a decrease of /Z/. After 6 months of immersion in HBSS, the behaviour of coated and uncoated substrates is similar as a consequence of particle dissolution. The corrosion resistance of titanium alloys results from the formation of a very stable and highly adherent oxide film onto the metal surface. This film is spontaneously formed when exposed to oxygen (even in traces) and it is able to reform in the event of damage. In most aqueous environments, TiO_2 forms, but it may also be a mixture of different oxides such as Ti_2O_3 and TiO.[39]

The third substrate employed was AISI 316L. While Ti and Cr alloys are widely used in permanent implants, AISI 316L is mostly employed in temporary devices. An extended electrochemical study has been conducted on this alloy with protective bioactive coatings, in order to follow its corrosion behaviour in long term applications in SBF, with the aim of lengthening its lifetime to permanent orthopaedic implants.

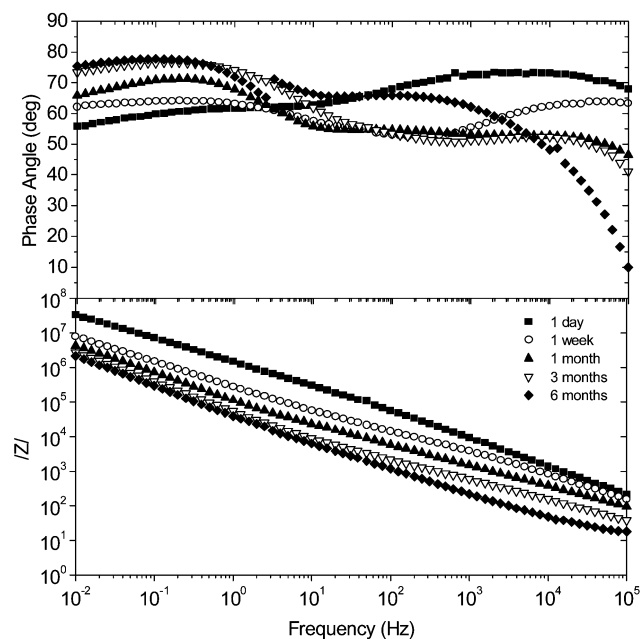Low sintering temperatures do not sensitise the metallic

substrates as demonstrated by Damborenea,[40] preserving the mechanical properties and avoiding the intergranular corrosion of the alloy.

Both single hybrid silica and double layered coatings with 10 wt% glass and glass-ceramic bioactive particles were deposited and studied. Fig. 5 shows the potentiodynamic curves for a pure silica coat and a double-layer coating compared with the uncoated stainless steel. Both coatings reduce the passive current density (i_{pass}) by more than three orders of magnitude with respect to the substrate; E_r reaches values as high as 1.25 V/SCE, providing a wide passivity range. The potential breakdown (E_r) is higher than the pitting potential (E_{pitt}) for uncoated steel; a higher pitting resistance is therefore expected for coated samples. E_r values are related to the oxygen evolution in the metal/coating interface, from electrolyte that may be accessed through pores or diffusion through the film, which leads to blistering of the coating. The very low i_{pass} indicates a small defect size and low density of defects in the coating, and thus an exposed metallic surface area three orders of magnitude lower than that of the uncoated metal.

Glass-ceramic coatings applied onto hybrid silica show anomalous behaviour with time. After 10 days of immersion, the samples have lower current densities than after 24 hours, possibly due to the blocking of pores with HA as a result of the reaction between glass-ceramic particles with SBF (not shown). This behaviour suggests that dissolution products are impeding the electrochemical process at the pores or defects of the coating, acting as a protective layer against corrosion and ion diffusion. In addition, these products promote further deposition of a semi-crystalline HA rich layer that can stimulate the primary stabilization of the implant.

The evolution of coatings with time was followed by EIS. Fig. 6 presents the behaviour of a double-layer coating with 10 wt% of glass particles, with respect to bare substrate. Two time constants become apparent after only three days of immersion in HBSS. The simultaneous appearance of a breakdown frequency, f_{break}, and its shifting to higher frequencies with immersion time indicate a progressive increase of the defective area. The external coat containing glass particles induces a higher defect density in the coating in comparison to hybrid silica. However, the response in the low frequency region indicates a diffusion controlled mechanism, and hence substrate attack remains negligible. Fig. 7 compares the EIS spectra of bare and coated AISI 316L after six months of immersion. The metal presents a pure capacitive response while both coated samples continue to show a diffusion controlled

Fig. 4 EIS spectra of Ti-6Al-4V alloy with monolayer coating with 10 wt% glass particles. Evolution with immersion time: (■) 1 day, (○) 1 week, (▲) 1 month, (▽) 3 months, (♦) 6 months.
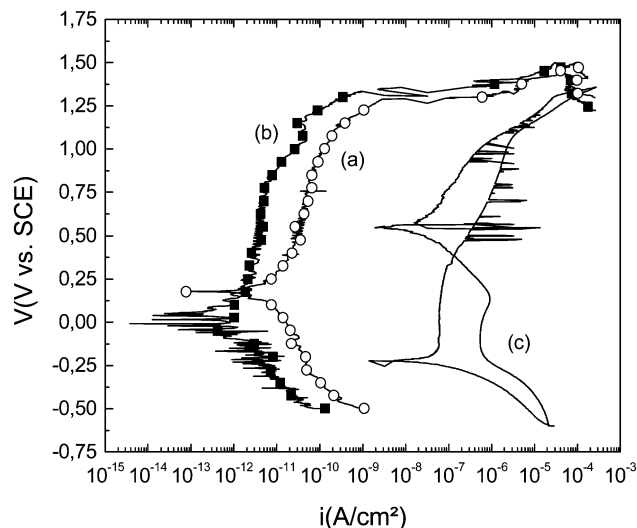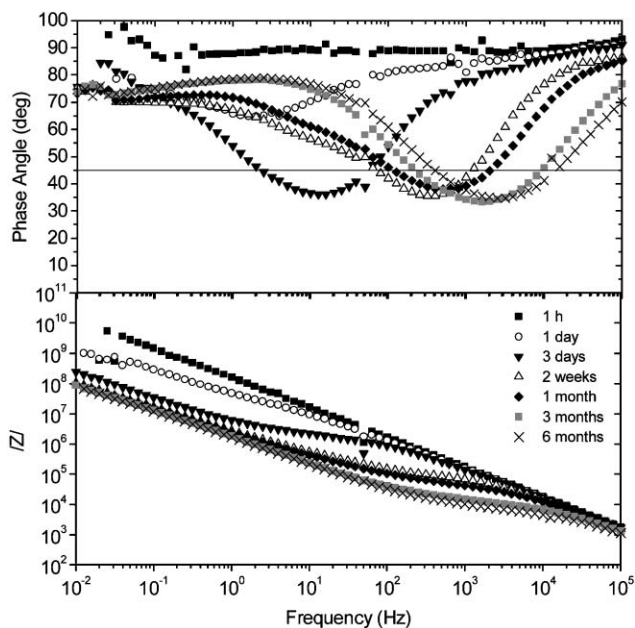
Fig. 6 EIS spectra of AISI 316L coated with a double layer coating with 10%wt glass particles. Evolution with time: (■) 1 h, (○) 1 day, (▼) 3 days, (▽) 2 weeks, (♦) 1 month, (■) 3 months, (×) 6 months.

mechanism, indicating that the barrier effect of the films remains unaltered for such long times.

3.3. *In vitro* assays

For an artificial material, the most essential requirement for bonding to a living tissue is the natural generation of bone-like apatite on its surface in the physiological environment. An initial evaluation of the bone-bonding ability of a material may be obtained by *in vitro* experiments in which surface formation of apatite is examined in a simulated body fluid.[13] Deposition of HA was followed by FTIR, a method sensitive to the vibration modes which are characteristic for molecular constituent groups, permitting the detection of HA and its growth on the material surface.[41–43] FTIR and XRD were used to follow the growth of apatite with time and as a function of the
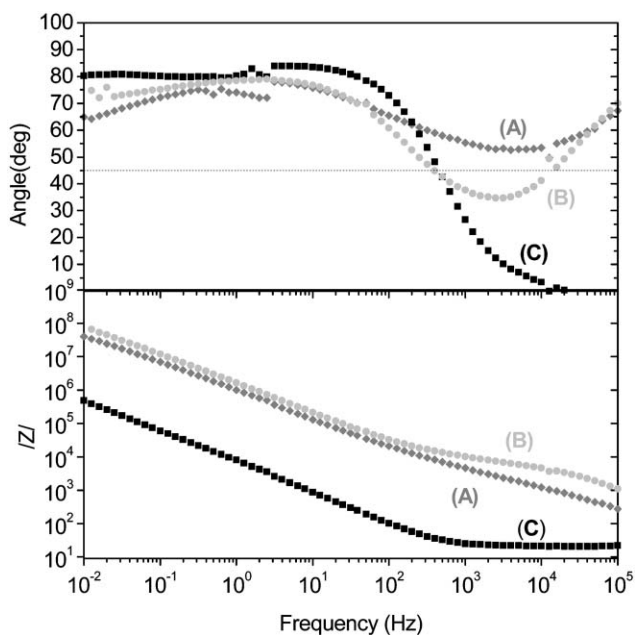

Fig. 7 EIS spectra of AISI 316L coated with: (a) hybrid single silica coating; (b) double-layer coating with 10 wt% glass particles, compared with bare material (c).

type and concentration of particles, the particle size and the thickness of the coating. The deposition of HA was similar for glass and glass-ceramic particles of the same concentration. The deposition rate is faster for higher concentrations, lasting from 7–10 days for coatings with 5 wt% glass to less than 3 days for coatings containing 10 wt% glass or glass-ceramic particles. The deposition kinetics also depends on particle size, with faster rates observed for smaller powders. No relationship with the coating thickness could be determined.

Fig. 8 shows a micrograph of a double layer with 10 wt% glass particles onto AISI 316L after one week of immersion. Deposition and crystal growth were followed by the increment of the corresponding FTIR signals. As XRD pattern obtained after 7 days of immersion in HBSS showed peaks corresponding to crystalline apatite; the low intensity is probably due to the expected low crystallinity of the HA deposit. Similar results were obtained for the other studied alloys.

3.4. Ion release

One of the concerns about surgery alloys is the potential toxicity of the metals ions that can be released in the body environment. Sol–gel coatings were formulated to serve not only for the primary stabilisation of the tissue but also as a barrier to release of ions.

ICP and ICP-MS were carried out for the different alloys. The Co-base alloy showed a concentration of Co ions more than one order of magnitude lower after 30 days of immersion when coated with double-layer coatings with bioactive glass-ceramic particles, indicating the barrier effect of these coatings against diffusion. Cr diffusion is lower still, being under the detection limit of the equipment.

ICP-MS has been used for characterising as-received and coated AISI 316L samples for immersion times of up to one year. This technique permits concentrations in the level of ng mL^{-1} to be detected. For Cr, Ni and Mo ions the detection limit is about 1 ng cm^{-2}. From tests performed at 5 and 37 °C, no Mo ions were detected after 12 months of immersion. Fig. 9 shows the behaviour of released Ni as a function of time for bare and coated steel. All the coatings seem to act as barriers against diffusion, with the best effects observed for hybrid silica and double-layer coatings with glass particles. Similar behaviour is observed for Cr diffusion. After longer immersion times, the behaviour of the hybrid silica and double-layer coatings is similar, confirming the results obtained from electrochemical measurements.[35] The single glass particles containing coatings have higher ion diffusion. This is likely resulting from partial dissolution of the particles that creates flaws and pores, allowing the fluid to come in contact with the substrate. In contrast, a coat of hybrid silica, alone or as first coat in double-layer films, shows a prolonged protecting barrier effect.

Using the ^{57}Fe isotope of iron, free from isobaric interferences, results in a higher detection limit of around 10 ng cm^{-2}. Under these conditions, only the pure hybrid silica coatings can be considered as an effective barrier against diffusion. The glass and glass-ceramic bioactive particles, melted using low Fe containing sand, are partially dissolved when immersed in SBF, masking the detected Fe values. Further work is in process to study this problem.

The diffusion results obtained by ICP-MS suggest that sol–gel coatings act as diffusion barriers reducing the release of ions and preventing the possibility of biotoxicity.

3.5. *In vivo* assays

Preliminary short-time subcutaneous *in vivo* tests were carried out to determine the influence of implants during the first stages of healing. The main objective of these assays was to detect possible rejection reactions of living tissues with AISI 316L
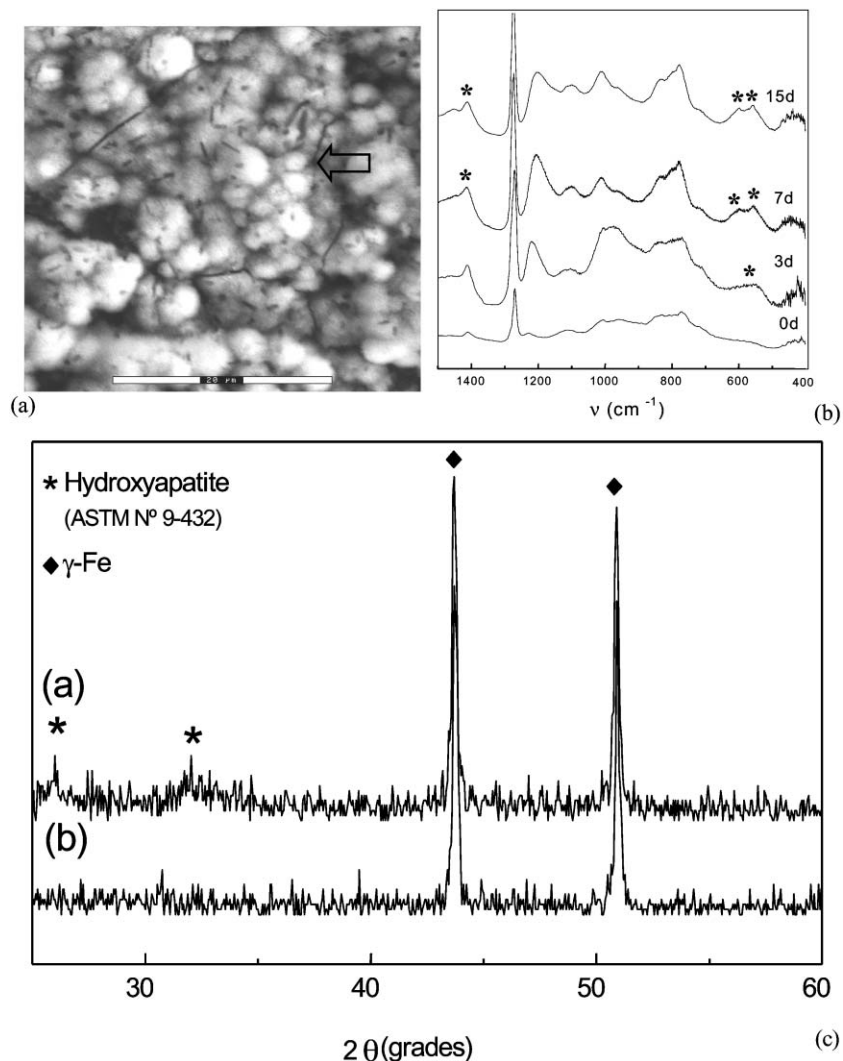
Fig. 8 (a) Hydroxyapatite (HA) deposited onto a double-layer coating with 10 wt% glass particles after 1 week of immersion in HBSS, at 37 °C. (Bar = 20 μm); (b) FTIR spectra of the same coating after different soaking times in HBSS; bands corresponding to apatite are indicated; (c) XRD patterns of the deposit formed on the double layer coating before (b) and after (a) 1 week of immersion. HA and Fe peaks are indicated.

samples coated with hybrid silica and with bioactive glass containing films, compared with the bare substrates. After one month of implantation, it was noticed that although both coated samples promote the formation of a fibrous capsule around the implant, this capsule is much thinner for the sample with the particle containing coating. No evidence of corrosion and better tissue–implant interaction in the samples coated
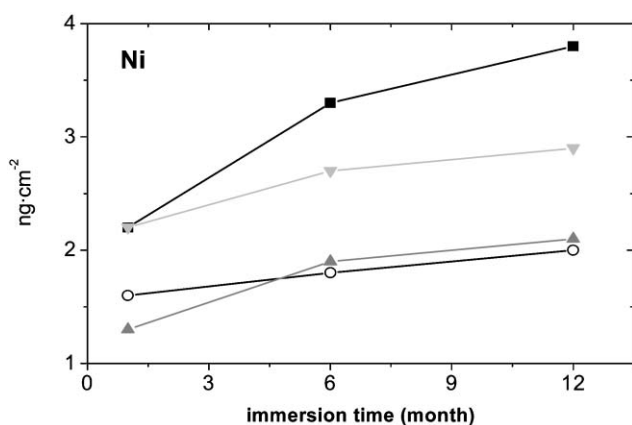

Fig. 9 Ni ions release as a function of time for AISI 316L: (■) uncoated, (○) hybrid coating and (▼) mono and (▲) double-layer coatings containing 10 wt% glass.

with HS and with particle containing films with respect to the uncoated steel were observed; the possibility of a negative response from soft tissues may, therefore, be excluded.[35]

The interaction between osseous tissue and sol–gel coating was studied by the press fit technique. All five animals used in the *in vivo* endomedular study were ambulatory for 24 h post-operation and showed predisposition for feeding and healing of wounds in both legs. None of the implants became clinically infected and no signs of infection or displacement of any of the samples were observed during the study.

Fig. 10 shows an X-ray of one of the animals after 53 days of implantation. Fig. 11 presents a micrograph of tissue that was in contact with CrCoMo alloy covered by a double sol–gel coating with 10 wt% glass-ceramic during the same implant period (200× magnification). Well conserved muscular tissue in the peripheries and spicules of osseous tissue were observed for all the samples; the tissue did not, therefore, appear to be affected by the metallic implant. A new lamellar histionic structure with plexiform features made of collagen tissue (non-mineralised) and vascular development is observed. As this new tissue showed extensive vascularity, it is possible that the tissue is growing with an osteoid structure. In contrast, all the uncoated wires showed poor vascularity in the new tissue (Fig. 12). It is, thus, reasonable to assume that this tissue structure is less effective for enhancement of bone growth.[38]

These results are encouraging with respect to the potential of sol–gel coatings on improving the osseo-integration of the
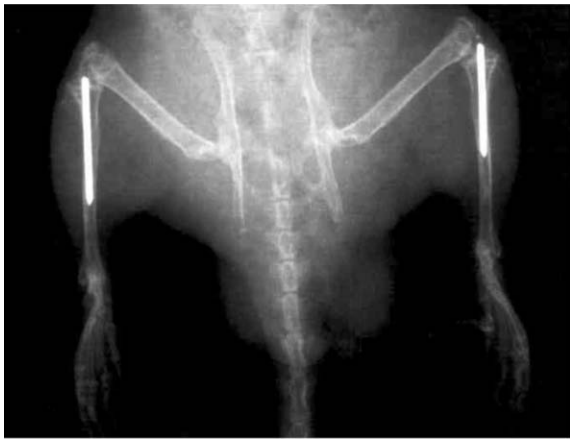
Fig. 10 X-Ray of one of the animals 53 days after implantation.

Fig. 12 Photograph of tissue that was in contact with bare CrCoMo (400 × magnification).

metallic implants. *In vivo* assays are also in progress for titanium and stainless steel alloys. Bigger animals (rabbits) and longer implantation times (up to six months) are being employed in order to evaluate bone regeneration and the implant/bone adhesion around coated samples.

4. Conclusions

Continuous and defect-free hybrid sol–gel coatings were obtained on surgery alloys. The incorporation of bioactive glass or glass-ceramic particles on the surface promoted bioactivity.

Electrochemical characterisation of samples coated with mono and double-layer coatings showed a dramatic reduction of the passive current densities compared with the bare alloys. The coatings improved the protection potential of the base materials in the tested electrolytes. EIS results for immersion times of up to six months demonstrated the stability of the coatings and the prevention of electrolyte penetration.

In vitro response was fast and dependent on the concentration and size of particles but not on the thickness of the coating. HA deposits of low crystallinity were observed for all the coated alloys after 3–7 days of immersion in SBF or HBSS.

Sol–gel coatings act as diffusion barriers, strongly impeding ion release and avoiding biotoxicity.

In vivo tests showed no rejection reactions or inflammatory response. Endomedullar implants of Co alloys wires coated with double-layer coatings containing glass-ceramic particles exhibited newly formed bone with considerable vascular development, which was not observed in the as-received wires.
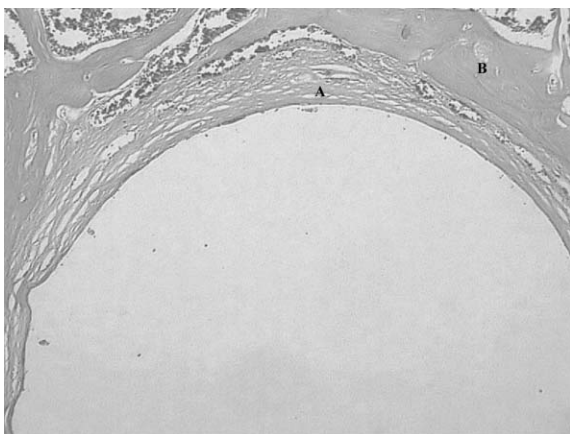

Fig. 11 Photograph of tissue that was in contact with CrCoMo alloy coated with a double-layer coating with 10 wt% of glass-ceramic particles. The new lamellar histionic structure with vascular development is marked as **A** and the osseous tissue as **B** (200 × magnification).
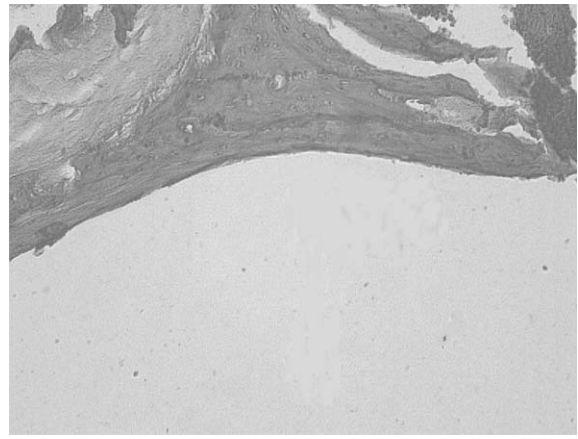
The promising results presented in this work suggest that bioactive particle containing sol–gel coatings are able to enhance early fixation due to the formation of HA deposits and neo formed vascular-rich osseous tissue in the tissue–coating interface. Devices coated with this technology should provide not only a better corrosion resistance than uncoated implants, with substantial reduction of the quantity metal ion release to the body, but also provide a substrate for ingrowth and bone attachment. They are thus suitable for permanent implants.

The excellent electrochemical performance of coated AISI 316 L steel in simulated body fluids demonstrates its suitability for use in permanent orthopaedic appliances, providing a competitive alternative related to Co and Ti alloys. The minimum ion release and the absence of rejection reactions are further benefits of this material.

Hybrid pure silica coatings are instead recommended for temporary devices where superior corrosion resistance and a barrier to metal ion diffusion are expected. Direct bonding between the implant and the tissue is thus avoided. The better tissue–implant interaction of the coated samples with respect to the uncoated ones with no evidence of rejection is a further advantage of these coatings.

5. Acknowledgements

6. References

1 J. J. Jacobs, J. L. Gilbert and R. M. Urban, *J. Bone J. Surg.*, 1998, **80A, 2**, 268–282.
2 Ying-Sing Li, Kang Wang, P. He, Bill Huang and Paul Kovacs, *J. Raman Spectrosc.*, 1999, **30**(2), 97–103.
3 S. Lee, F. Brennan, J. Jacobs, R. Urban, D. Ragusa and T. Glant, *J. Orthop. Res.*, 1995, **15**, 40–95.
4 M. Niinomi, D. Kuroda, K. Fukunaga, M. Morinaga, Y. Kato, T. Yashiro and A. Suzuki, *Mater. Sci. Technol.*, 1999, **A263**, 193–199.
5 M. A. Khan, R. L. Williams and D. F. Williams, *Biomaterials*, 1996, **17**, 2117–2126.
6 G. Wintere, *J. Biomed. Mater. Res. Symp.*, 1974, 11.
7 Metals handbook, Ninth Edition, *Corrosion*, **vol. 13**, ASM International, Metals Park, Ohio, 1987, 1324.
8 L. Hench, *J. Am. Ceram. Soc.*, 1991, **74**, 1487.

9   J. Gültij, M. Brich, H. Hämnerle and W. Nisch, *J. Mater. Science: Mater. Med.*, 1994, **5**, 463.
10 C. Larsson, P. Thomsen and B. Aronsson, *Biomaterials*, 1996, **17**, 605.
11 M. Urban, J. Jacobs and D. Sumner, *J. Bone J. Surg.*, 1996, **78A**, 1068.
12 M. Jasty, C. Bragdon, T Haire, R. Mulroy and W. Harris, *J. Biomed. Mater. Res.*, 1993, **27**, 639–644.
13 T. Kokubo, H. Kushitani, S. Sakka, T. Kitsugi and T. Yamamuro, *J. Biomed. Mater. Res.*, 1990, **24**, 721–734.
14 C. G. Pantano, A. E. Clark and L. L Hench, *J. Am. Ceram. Soc.*, 1976, **59**, 37.
15 T. Kokubo, *J. Non-Cryst. Solids*, 1990, **120**, 138.
16 M. Pereira, A. Clark and L. Hench, *J. Am. Ceram. Soc.*, 1995, **78**, 2463.
17 M. Pereira and L. Hench, *J. Sol-Gel Sci. Technol.*, 1996, **7**, 59.
18 S. Cho, F. Miyagi, T. Kokubo, K. Nakanishi, N. Soga and T. Nakamura, *J. Ceram. Soc. Jpn.*, 1996, **104**, 399.
19 O. De Sanctis, L. Gómez, N. Pellegri, C. Parodi, A. Marajofsky and A. Durán, *J. Non-Cryst. Solids*, 1990, **121**, 338.
20 J. J. de Damborenea, N. Pellegrini, O. de Sanctis and A. Durán, *J. Sol-Gel Sci. Technol.*, 1995, **4**, 239.
21 P. Galliano, J. J. de Damborenea, M. J. Pascual and A. Durán, *J. Sol-Gel Sci. Technol.*, 1998, **13**, 723–727.
22 Fillaggi, Pillar, *Evaluating sol-gel ceramic thin films for surface modification of metallic implants: film adhesion and the ZrO_2/Ti_6Al_4V system*, 21st Annual Meeting of the Society for Biomaterials, 1995.
23 J. Gallardo, R. Moreno, P. Galliano and A. Durán, *J. Sol-Gel Sci. Technol.*, 2000, **19**, 107–111.
24 S. Sakka, *J. Sol-Gel Sci. Technol.*, 1994, **2**, 451.
25 M. Guglielmi, *J. Sol-Gel Sci. Technol.*, 1997, **8**, 443.
26 D. R. Uhlmann and G. Teowee, *J. Sol-Gel Sci. Technol.*, 1998, **13**, 153.
27 L. Hench, in *Bioceramics: Material Characteristics vs. In Vivo behavior*, P. Ducheyne and J. Lemons, eds., Annals NY Acad. Sci., **523**, 1988, p. 54.
28 R. Li, A. E. Clark and L. Hench, *J. Appl. Biomater.*, 1991, **2**, 231.
29 P. Li, C. Ohtsuki, T. Kokubo, K. Nakanishi, N. Soga, T. Nakamura and T. Yamamuro, *J. Am. Ceram. Soc.*, 1992, **75**, 2094.
30 M. M. Pereira, A. E. Clark and L. L. Hench, *J. Biomed. Mater. Res.*, 1994, **18**, 693.
31 L. L. Hench, D. Wheeler and D. Greespan, *J. Sol-Gel Sci. Technol.*, 1998, **13**, 245.
32 J. Perez-Pariente, F. Balas and M. Vallet-Regi, *J. Biomed. Mater. Res.*, 1999, **47**, 170.
33 S. Cho, F. Migayi, T. Kokubo, N. Soga, C. Ohtsuki and T. Nakamura, *J. Biomed. Mater. Res.*, 1996, **33**, 1451.
34 C. J. Brinker and G. W. Scherer, *Sol Gel Science: The Physics and Chemistry of Sol-Gel Processing*, Academic Press Inc., San Diego (USA), 1990, p. 798.
35 J. Gallardo, P. Galliano and A. Durán, *J. Sol-Gel Sci. Technol.*, 2001, **21**, 65–74.
36 T. Chartier, E. Streicher and P. Boch, *Am. Ceram. Soc. Bull.*, 1987, **66**, 653.
37 C. García, R. Moreno and A. Durán, Sent to *J. Sol-Gel Sci. Technol.*, 2003.
38 J. Ballarre, J. C. Orellano, C. Bordenave, P. Galliano and S. Cere, *J. Non Cryst. Solids*, 2002, **304**, 279–286.
39 Metals handbook, Ninth Edition, *Corrosion*, **vol. 13**, ASM International, Metals Park, Ohio, 1987, 670.
40 J. J. Damborenea, N. Pellegri, O. De Sanctis and A. Durán, *J. Sol-Gel Sci. Technol.*, 1995, **4**, 239.
41 B. O. Fowler, *Inorg. Chem.*, 1974, **13**, 194.
42 R. F. Le Geros, G. Bone and R. Legeros, *Calcif. Tissue Res.*, 1978, **26**, 11.
43 D. G. A. Nelson and J. D. B. Feathestone, *Calcif. Tissue Int.*, 1982, **34**, 869.